

Gold nanoparticle enhanced surface plasmon resonance imaging of microRNA-155 using a functional nucleic acid-based amplification machine

Ke Zeng¹ · Hongyuan Li² · Yinyin Peng¹

Received: 14 January 2017 / Accepted: 19 April 2017 / Published online: 28 April 2017
© Springer-Verlag Wien 2017

Abstract MicroRNAs (miRNAs) are considered as being promising biomarkers for hematological malignancies, their aging, progression and prognosis. The authors have developed a method for the detection of miRNA-155 by using surface plasmon resonance (SPR) imaging coupled to a nucleic acid-based amplification strategy using gold nanoparticles (AuNPs). The target miRNA-155 is captured by surface-bound DNA probes. After hybridization, DNA-AuNP are employed for signal amplification via DNA sandwich assembly, resulting in a large increase in the SPR signal. This method can detect miRNA-155 in concentrations down to 45 pM and over dynamic that extends from 50 pM to 5 nM. The assay is highly specific and can discriminate even a single base mismatch. It also is reproducible, precise, and was successfully applied to the determination of miRNA-155 in spiked real samples where it gave recoveries in the range between 86% and 98%. This biosensor provides an alternative approach for miRNA detection in biomedical research and clinical diagnosis, which is highly effective and efficient.

Keywords Biosensor · Strand displacement amplification · Hematological malignancies · Gold nanoparticles · Molecular beacon · Enzymatic amplification · Clinical molecular diagnostics · Polydimethylsiloxane · Gold island array microchips · DNA hybridization

Introduction

MicroRNAs (miRNAs) are short, endogenous, single-stranded RNA molecules (18–23 nucleotides), which can regulate the gene expression in many cellular processes, such as cell proliferation, differentiation and tumor genesis [1, 2]. Since the discovery of miRNA in circulation, a large amount of miRNA-related biological studies have confirmed that each miRNA can affect numerous target mRNAs [3] and each mRNAs can be targeted by multiple miRNAs, enabling wide regulatory complexity of gene expression adjustment [4]. MiRNA-155 is encoded from the B cell integration cluster locus and is up regulated in cancer and inflammation [5]. Loss of canonical Notch signaling induces direct up regulation of miRNA-155 expression on bone marrow stromal and endothelial cells, which causes significant alterations of hematopoiesis. Moreover, miRNA-155 has been detected not only in the overall growth process of malignancy, but also the treatment of hematological malignancies. This indicates the important regulatory role that miRNA-155 has, as it participates both in expressional regulation of fundamental hematopoietic oncogenes and tumor suppressor genes. Therefore, miRNA-155 has been regarded as a diagnostic and prognostic biomarker in hematological malignancies and solid malignancies [6]. As a result, a simple and reliable assays for the detection of miRNA-155 is urgent for early diagnose and treatment of hematological malignancies. Conventional methods have been invented to sense miRNA, including Northern blotting

Electronic supplementary material The online version of this article (doi:10.1007/s00604-017-2276-2) contains supplementary material, which is available to authorized users.

✉ Yinyin Peng
pengyinyin802320@163.com

¹ Department of Hematology, The First Affiliated Hospital of Chongqing Medical University, Chongqing 400016, China

² Chongqing Key Laboratory for Advanced Materials and Technologies of Clean Energies, Southwest University, Chongqing 400715, China

[7], microarray [8], and quantitative real-time PCR (qRT-PCR) [9]. These established methods have some drawbacks in practical applications, i.e., semi-quantitative, laborious, and requiring expensive equipment [10]. To detect miRNA accurately is still a challenge due to its tiny size, low abundance, and sequence homology.

Various robust biosensing strategies for miRNA have been proposed, such as electrochemical [11], bioluminescence [12], electrochemiluminescence [13], colorimetry [14], Raman spectroscopy [15], and surface plasmon resonance (SPR) [16, 17]. Among these methods, SPR biosensors, measuring the change in refractive index near the sensing surface arisen from complex formation or dissociation [18], is an advanced technology to implement in-situ detection of biological molecule in real time. SPR imaging (SPRi) is able to extract the information of biological interactions from the change in the pixel intensity caused by the association and dissociation. Parallel analysis of interactions taking place at several locations on the sensing surface can be analyzed from the spatially resolved functionalized surface [19]. In this way, both sensorgrams (i.e., resonance signal vs. time) and real-time images of the sensor chip can be simultaneously recorded for high throughput analysis [20]. However, the direct SPR detection is not satisfying certain cases due to the sensitivity, especially for the detection of trace substance in complex biological samples. This has limited the further application of SPR. In order to overcome this shortcoming, more and more amplification strategies have been proposed by circulation amplification to directly enhance the SPR signal, including PCR [21], hybridization chain reaction (HCR) [22], rolling circle amplification RCA and nanoparticle enhancement [23]. Among these amplification technologies, strand displacement amplification (SDA), which can provide exponential amplification of a trace of DNA or RNA [24], has attracted more and more attention due to its fast, efficient, and no special equipment requirement [25]. Therefore, the SDA technology is believed to be a suitable strategy to implement simply determination of miRNA combined with SPR technology to produce high sensitivity.

Here, we report on a simple and sensitive SPRi biosensor for the detection of miRNA-155 based on the functional nucleic acid-based amplification machine that can produce large amounts of trigger DNAs for further analysis. In this assay, we combined AuNP to enhance SPR signal and improve the sensitivity of our biosensors. The inherent properties of molecular beacon (MB) mediated strand displacement amplification and enzymatic amplification ensure high sensitivity and specificity of the designated target. This strategy exhibits excellent analytical performance toward miRNA detection, which provides a promising sensing platform for the bioanalysis and clinical molecular diagnostics.

Experimental

Materials and reagents

Klenow fragment polymerase (3'-5' exo), Nb.BbvCI, dNTP and RNase inhibitor were purchased from New England Biolabs (USA). MiRNAs were obtained from TaKaRa Biotech. Inc. (Dalian, China, <http://www.takara.com.cn/>). HPLC-purified DNA oligonucleotides, bovine serum albumin (BSA), salmon sperm DNA were synthesized by Sangon Biotechnology Co. Ltd. (Shanghai, China, <http://www.sangon.com/>). H₂AuCl₄ was purchased from Sinopharm Chem Ltd. (Shanghai, China, <http://www.sinoreagent.com/>). Polydimethylsiloxane (PDMS) were obtained from Sigma-Aldrich (St Louis, MO, USA, <http://www.sigmaaldrich.com/>). The sequences of nucleic acids employed in this study were shown in Table 1. All oligonucleotides were dissolved in triethylene-diaminetetraacetic acid (TE) buffer (pH 8.0, 10 mM Tris-HCl, 1 mM EDTA) and stored at -20 °C, which were diluted in appropriate buffer prior to use. All solutions and deionized water were treated with diethylprocarbonated (DEPC) and autoclaved to protect from RNase degradation. All other reagents were of analytical grade, and Millipore-Q water ($\geq 18 \text{ M}\Omega\text{-cm}$) was used in all experiments. Running buffer (pH = 7.4) contained 30 mM Na₃PO₄, 450 mM NaCl, 3 mM EDTA, 0.25% triton $\times 100$.

Apparatus

A home-made SPRi sensor platform (Fig. 1a) was developed to investigate the hybridization of DNA. This Kretschmann geometry based SPRi sensor is combined with gold island array microchips. Briefly, the BK7 glass array substrate coated with gold was mounted on an optical stage containing a PDMS flow cells, with a dimension of 15 mm \times 4 mm \times 1 mm and a volume of 60 μL . A refractive index matching liquid ($n = 1.610$) is mediated between the array substrate and the equilateral SF2 triangular prism ($n = 1.616$). The optical stage was fixed on a goniometer that allows to tune the incident angle. A red light emitting diode (LED, 650 nm) was used to excite the surface plasmon resonance and the reflected images were captured by a CCD camera. The injection of sample solutions into the flow cell was monitored in real time by recording the changes in reflectance at every 20 s. This sensorgram was analyzed using a home-built program. UV-VIS spectra were carried out on a UV2550-VIS spectrophotometer (Shimadzu, Japan). Transmission electron microscopic (TEM) image was carried out using an H-7500 transmission electron microscope (Hitachi,

Table 1 DNA sequences employed in this work

Oligonucleotide	Sequence (5'-3')
Target miRNA-155	UUA AUGCUAAUCGUGAUAGGGGU
NC (miRNA-21)	UAGCUUAUCAGACUGAUGUUGA
One-base mismatch target	UUA AUGCUAAU <u>A</u> GUGAUAGGGGU
Double-base mismatch target	UUA AU <u>A</u> CUAAU <u>A</u> GUGAUCGGGGU
MB	GTCAGATGAATTCGTGTGAGAGCACCTCAGCCGCGCG ACCCCTATCACGATTAGCATTAAGTCGCGCGCCCCC
Capture probe	SH-(CH ₂) ₆ -TTTTTGTGAGATGAATTCG
Detection probe	TGTGAGAGCACCTTTTT-(CH ₂) ₆ -SH

NC non-complementary mismatched miRNA-21, MB molecular beacon with C₆ SPACER protected 3'-end

Japan). Gel images were recorded on an imaging system (Bio-Rad Laboratories, USA).

Preparation of AuNPs and DNA-functionalized AuNPs

AuNPs were prepared according to the literatures [26]. 4 mL of 1% trisodium citrate was added to 100 mL of boiling 0.01% HAuCl₄ solution, stirring rapidly and boiling for 15 min. The solution turned deep red, indicating the formation of AuNPs. Then the resulting Au colloidal solution was cooled to room temperature with continued stirring and stored at 4 °C until use.

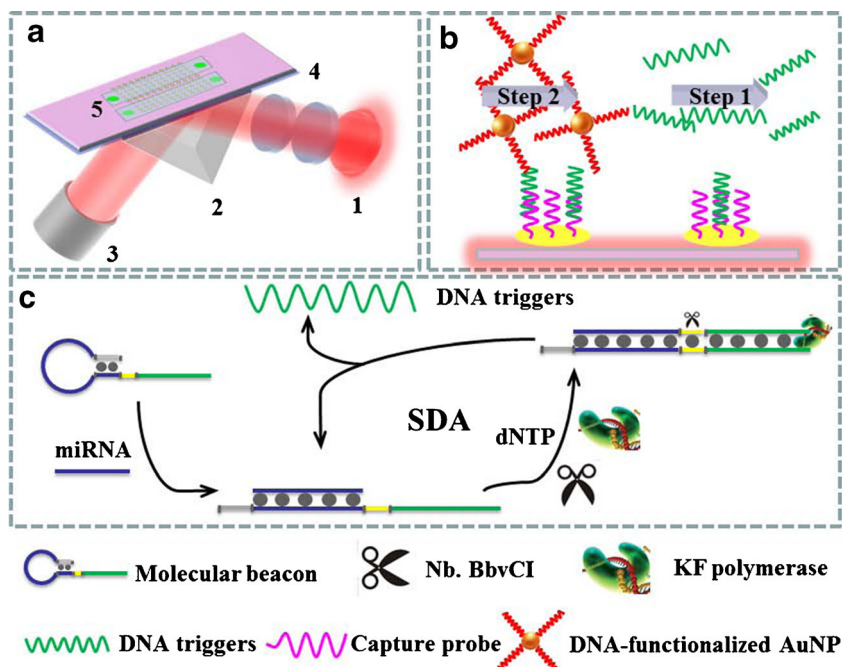
The DNA-functionalized AuNPs were achieved by adding 90 μL of 100 μM DNA probes into 3 mL of AuNP solution [27]. After incubating for 12 h at 4 °C with slight stirring, the DNA-AuNP conjugates were “aged” in 0.5 M NaCl for another 12 h. Finally, the solution was centrifuged at 9900×g for 30 min to

remove the excess reagents. The red precipitate was washed, centrifuged and dispersed in hybridization buffer for future use.

Preparation of the SPRi biosensor

Prior to capture probe immobilization, the bare gold chip was cleaned with fresh piranha solution for 5 min to eliminate adsorbed organic impurities. Then, the pretreated gold chip was washed thoroughly with Milli-Q water and pure alcohol, followed by drying under nitrogen. 200 μL of 1 μM thiolated capture probes in TE buffer was dropped on the pretreated gold chip surface and incubated 2 h at room temperature. After being washed with the washing buffer (20 mM Tris-HCl, 100 mM NaCl, 5 mM MgCl₂, 0.05% Tween-20), the chip was immersed into 1 mM MCH for 1 h to obtain well-aligned DNA monolayer which occupied the left bare sites. The chip was further rinsed with the washing buffer and

Fig. 1 **a** Schematic of SPRi system combined with gold islands microarray. 1. 650 nm LED light. 2. BK7 triangular prism. 3. CCD camera. 4. The gold island microarray chip (with 10 × 10 gold islands) 5. PDMS flow cell with inlet channel and outlet channel, **b** Cartoon representation of DNA triggers and DNA-AuNP hybridization onto gold microarray spots and **c** Schematic illustration of functional nucleic acid-based amplification machine for miRNA detection



treated in 1% BSA and $125 \mu\text{g}\cdot\text{mL}^{-1}$ salmon sperm DNA for 30 min to block the nonspecific binding sites and enzyme on its surface. After washing, the chip was allowed to dry and docked into the instrument for experiment.

Assay protocol for target miRNA

The SDA reaction was initiated by adding $3 \mu\text{L}$ target miRNA with different concentrations of reagents. They are $6 \mu\text{L}$ of 10 nM MB probes, $0.6 \mu\text{L}$ of $0.1 \text{ U}\cdot\mu\text{L}^{-1}$ Klenow fragment, $0.6 \mu\text{L}$ of $0.2 \text{ U}\cdot\mu\text{L}^{-1}$ Nb.BbvCI, $0.7 \mu\text{L}$ of $250 \mu\text{M}$ dNTP, $0.9 \mu\text{L}$ of $1.2 \text{ U}\cdot\mu\text{L}^{-1}$ RNase inhibitor, $3 \mu\text{L}$ NE Buffer 2, $3 \mu\text{L}$ CutSmart™ Buffer and $12.2 \mu\text{L}$ DEPC-treated water respectively. Then the mixtures of SDA reaction were incubated at $37 \text{ }^\circ\text{C}$ for 1.5 h. After the strand displacement amplification reaction, Klenow fragment (3'-5'exo) and Nb.BbvCI were inactivated by heating the reaction mixture at $65 \text{ }^\circ\text{C}$ for 10 min. The resulting mixture was diluted to be $300 \mu\text{L}$ with running buffer, and used in the following experiment or stored at $-20 \text{ }^\circ\text{C}$. Next, the mixture was injected into the flow cell (Step 1, Fig. 1b). The DNA triggers hybridized with the capture probes was immobilized on the gold chip surface at the flow rate of $0.02 \text{ mL}\cdot\text{min}^{-1}$ as showed in Fig. 1b and Fig. 2a. After being washed with the running buffer, DNA-functionalized AuNPs were then injected on the biosensor surface (Step 2, Fig. 1b) and hybridized with another part of DNA triggers for about 30 min. The sensor surface was regenerated with the regeneration solution (50 mM NaOH) at the flow rate of $0.04 \text{ mL}\cdot\text{min}^{-1}$ in order to remove the binding analytes on the gold film prepared for the next measurements. Three replicate tests were implemented and the average value was calculated. All experiments were carried out at room temperature about $25 \text{ }^\circ\text{C}$ (except where noted).

Results and discussions

Principle of functional nucleic-based amplification machine

The principle for miRNA detection is illustrated in Fig. 1c. The molecular beacon (MB) template consists of three domains, which are miRNA-binding domain, recognition domain for nicking by Nb.BbvCI, and amplification domain for producing DNA triggers respectively. The presence of target miRNA triggered the specific hybridization of miRNA in corresponding domain to open the MB template, which leads to a part duplex. Then, the target miRNA is extended along the template to form a complete duplex by Klenow fragment and dNTPs. Subsequently, the nicking enzyme can specifically recognize the duplex nicking site, cleave the upper extended DNA strand and expose a new replication site for polymerase. Thus, a number of DNA triggers are produced through the continuous circulation of extension, cleavage, and SDA. One part of DNA triggers can hybridize with capture probe immobilized on the gold chip, and the other part of DNA triggers hybridize with detection probe functionalized on AuNPs. The growing number of DNA triggers results in a great amplification of detection signal, which produces the enhancement of SPR signal for quantitative detection of miRNA at low concentration.

Choice of materials and characterization of biosensor fabrication

In the case of low analyte concentrations, extremely high analyte sensitivity is required. This would require large changes in the SPR wavelength in response to relatively small changes in the medium refractive index. The dependence of the SPR sensitivity on the metal type and the nanoparticle shape has been discussed by Lee and El-

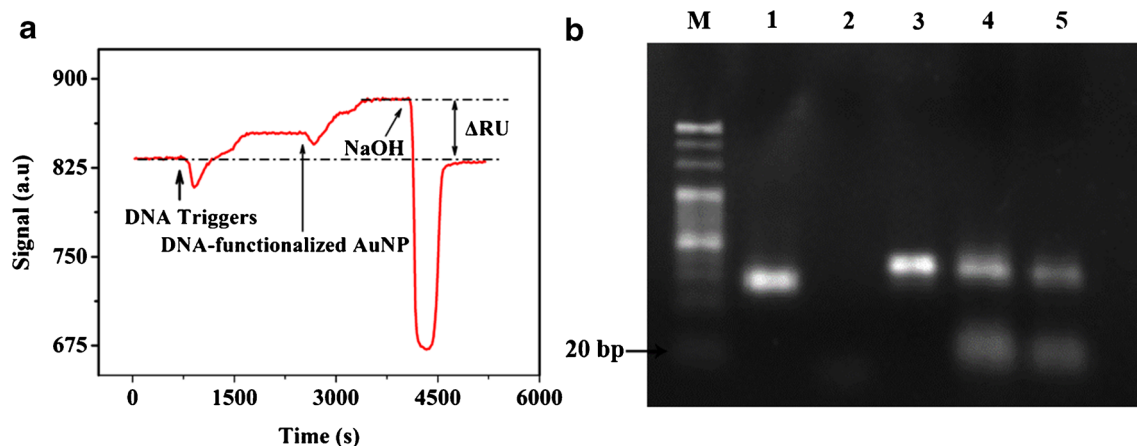
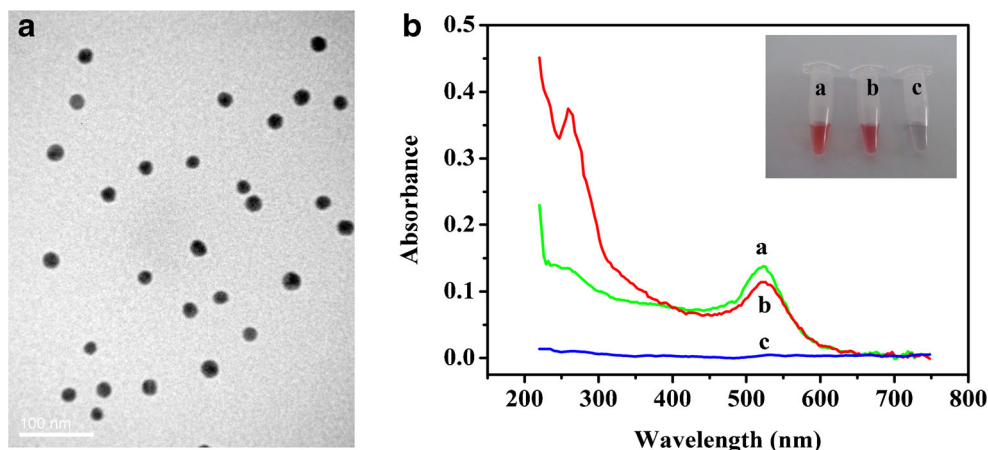


Fig. 2 a Typical SPRi sensorgram of DNA triggers hybridization, DNA-AuNP sandwich signal amplification. b The native PAGE analysis: M: 500 bp DNA Ladder Marker, lane 1: MB, lane 2: miRNA, lane 3: MB + miRNA, lane 4 and lane 5: SDA

Fig. 3 **a** TEM image of AuNPs. **b** UV-vis absorption spectra of (a) AuNPs, (b) AuNPs with SH-DNA after addition of 0.5 M NaCl, (c) AuNPs without SH-DNA after addition of 0.5 M NaCl



Sayed [28]. However, the choice of metals is limited to Ag and Au, both of which a similar wavelength dispersion, optical properties and intense electromagnetic fields. The extremely high extinction coefficients and the strongly distance-dependent optical properties of gold nanoparticles allow the nanoparticles to be utilized as ideal reporting groups. For example, the extinction coefficients of 13 and 50 nm gold particles are 2.7×10^8 and $1.5 \times 10^{10} \text{ M}^{-1}\cdot\text{cm}^{-1}$ (at $\sim 520 \text{ nm}$), respectively, which are 3–5 orders of magnitude more than those of traditional organic compounds [29]. In addition, the surface plasmon resonance is the coherent excitation of all the “free” electrons within the conduction band, leading to an in-phase oscillation. In gold nanoparticles, the surface and the bulk plasmon are coupled, and the charge density varies everywhere in the particle. The multipolar resonances exist for individual nanoparticles and can be excited [30], resulting SPR signal enhancement. So in our work, we chose AuNPs as signal-amplifier.

The TEM image of synthesized AuNPs is shown in Fig. 3a. Spherical AuNPs with an average diameter of 18 nm exhibited homogeneous dispersion. The DNA-

AuNP conjugates were confirmed by UV-VIS absorption spectra (Fig. 3b), which demonstrated that the successful labeling of thiol-modified oligonucleotides was achieved.

To verify whether the DNA triggers can be produced in the presence of MB and target miRNA, PAGE analysis was carried out. As shown in Fig. 2b, the distinct band of 27 nt, representing the DNA triggers, was observed with the addition of target miRNA (Fig. 2b, lane 4 and lane 5). However, the DNA triggers were not observed in the control group (Fig. 2b, lane 3), revealing that the MB/trigger DNA successfully produced the expected result.

The amplification characteristics were further evaluated by SPR measurements. As shown in Fig. 2a, the introduction of mixture led to an increase of SPR signal, which is attributed to the hybridization process. The SPR signal is continuously increased by the addition of DNA-functionalized AuNPs due to the accumulation of a large quantity of metallic particles assembled on the sensor surface. For comparison, the traditional sandwich assay can only detect introduced probe (Fig. S1). Without SDA signal amplification and enhancement of

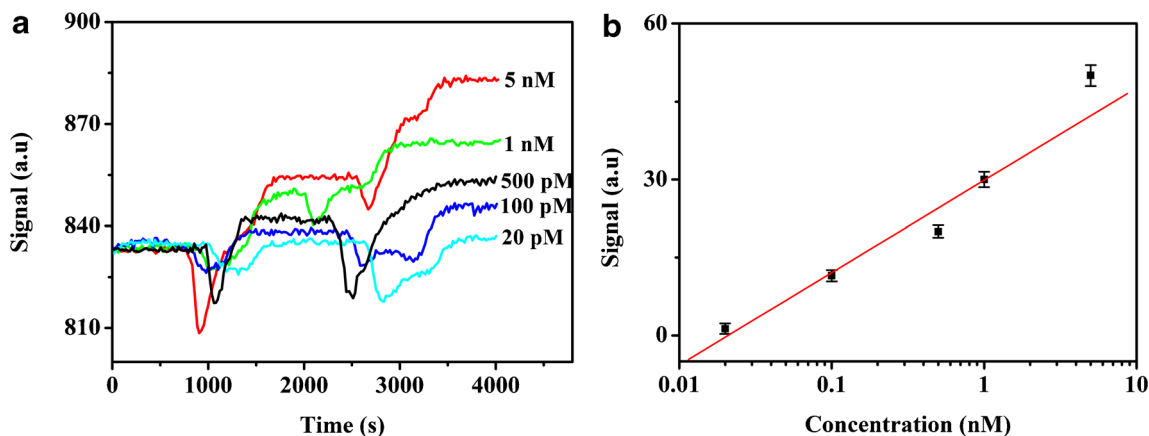


Fig. 4 **a** Typical SPRi sensorgram and **b** the corresponding calibration curve to 0.02, 0.1, 0.5, 1 and 5 nM of target miRNA with SDA amplification

Table 2 Comparison between the bioassay and other reported SPRi sensors for miRNA detection

Technique	Target	Method	Material	Limit	Reference
SPR	miRNA-122	SE	Streptavidin	1.7 fM	[31]
ECL	miRNA-21	HCR	Ru(phen) ₃ ²⁺	1 fM	[32]
Electrochemistry	miRNA-126	EM	Au, Ag nanoclusters, etc.	0.79 fM	[33]
Electrochemical	miRNA-222	SDA	--	40 pM	[34]
SPRi	ssRNA	T4	Silica nanoparticles	100 fM	[35]
SPRi (home-made)	miRNA-155	SDA	AuNP	45 pM	This work

SE Streptavidin-enhancement, ECL electrochemical luminescence, HCR hybridization chain reaction, EM electrode modified, PE photoelectrochemical, quantum dots, QDs; AuNP, gold nanoparticle; T4, T4 RNA ligase

AuNPs, produced SPR signal from the same experimental conditions was much smaller compared to the one employed with the signal enhancement strategy.

Optimization of method

Signal amplification plays a key role to improve the sensitivity of SPRi biosensor in this study. To achieve higher detection sensitivity, the following experimental parameters were optimized: (a) MB template concentrations; (b) the incubation time of the SDA reaction. Respective data and Figures are given in the Electronic Supporting Material (fig. S2). The SPR signal experiences a significant increase as the concentration of MB increasing from 1 nM to 10 nM. Then trend of SPR signal tended to be plateaus wherever the concentration of MB was increased to be 15 nM; As the incubation time increased, the signal sharply increased and reached a stable value at 90 min. Therefore, we found the following experimental conditions to give best results: (a) 10 nM MB; (b) 90 min incubation time.

Analytical performance of designed biosensor

Under the optimal experimental conditions, analytical performance of this SPRi biosensor was evaluated toward synthetic miRNA-155 standards at various concentrations. The SPR

signal increased with the increasing target miRNA-155 concentrations (Fig. 4). The plot of the response vs. the logarithm of miRNA-155 concentrations showed a good linear relationship in the range from 0.02 to 10 nM. The resulting linear equation expressed as Eq. (1) has a correlation coefficient of 0.9960 (Fig. 4b)

$$S = 29.87 + 17.78 \lg C_{\text{miRNA}} \quad (1)$$

where S is the SPR response signal, C_{miRNA} is the concentration of target miRNA. Additionally, the limit of detection (LOD) was estimated to be 45.45 pM at a signal-to-noise ratio (S/N) of 3. In order to further investigate the performance of the biosensor, the conventional triple-stranded hybridization was used for the comparison under the same condition. As shown in Fig. S1, the linear relationship between the DPV responses and the logarithm of DNA concentration was observed from 1 to 100 nM with a detection limit of 1.67 nM (at S/N = 3). As a result, the LOD of using SDA and enzymatic amplification is approximately 36 times higher than that of using the conventional triple-stranded hybridization. Compared with the reported colorimetric methods listed in Table 2, the biosensing strategy based on home-made SPRi did not exhibit any improvement in the analytical performance. But this method based on home-made SPRi provided

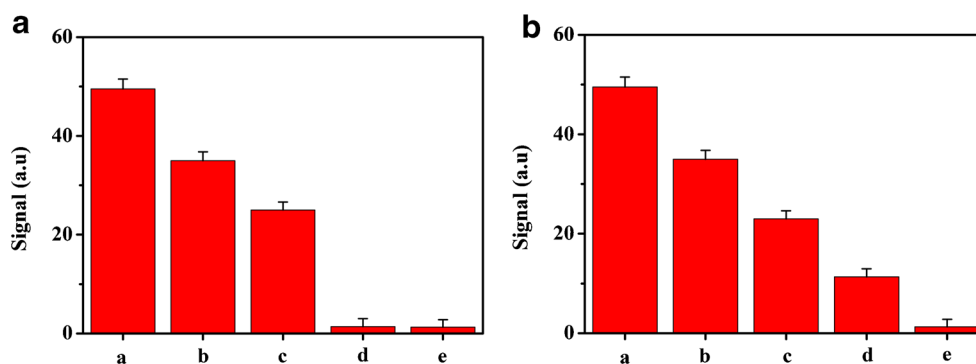


Fig. 5 a The SPR response signal for miR-155, single-base mismatch target (SM), double-base mismatch target (DM), non-complementary sequence (NC) and miR-21 at the concentrations of 5 nM, respectively. The error bars represent average standard errors for three measurements. b The SPR response signal for to blank (f), 100 pM miRNA-155 in the

serum samples (e), 500 pM miRNA-155 spiked into the serum samples of 100 pM miRNA-155 (d), 1 nM miRNA-155 spiked into the serum samples of 100 pM miRNA-155 (b), and 5 nM miRNA-155 spiked into the serum samples of 100 pM miRNA-155 (a)

technical support for high-throughput miRNA analysis. In addition, The achieved high sensitivity can be attributed to dual signal amplifications of molecular beacon mediated SDA and enzymatic amplification. Therefore, this SPRi biosensor might be applied to quantification of miRNA with a wide linear range and low detection concentration.

Specificity and reproducibility of the miRNA detection

To further evaluate the specificity of this biosensor, the complementary target (miRNA-155), the single-base mismatched miRNA-155 (SM), the double-base mismatched miRNA-155 (DM), the non-complementary mismatched miRNA-21 (NC) and a sample without target as a blank control were chosen as the models. Four different kinds of oligonucleotides were analyzed at the same concentration of 5 nM. As shown in Fig. 5a, the responses of the complementary target miRNA-155 were much higher than those of the other mismatch sequences, which indicated that the established biosensor displayed a high selectivity to discriminate perfectly complementary target and the mismatched miRNAs. In addition, to further evaluate the reproducibility of the SPRi biosensor, six different tests were prepared for the detection of 5 nM and 500 pM miRNA-155. The relative standard deviations (RSD) of six replicate measurements were 9.56% and 5.37%, respectively. The good specificity and acceptable reproducibility for the miRNA-155 detection have been exhibited by this established SPRi biosensor.

Real sample analysis

To estimate the analytical feasibility and promising application of the SPRi biosensor, we performed the miRNA assay using serum samples which were diluted to be 20% with DEPC treated water. Different concentrations of the synthetic miRNA-155 were spiked into the diluted serum samples. As shown in Fig. 5b, the signal generated by 100 pM, 500 pM, 1 nM, and 5 nM miRNA-155 in the diluted serum samples can be obviously distinguished from that generated by the blank. The recoveries were estimated to be in the range between 86% and 98%. This suggests that the performance of biosensor was not affected in complex mixtures and the established strategy might a potential tool for miRNA assay in real biological samples.

Conclusions

In summary, we have successfully developed a rapid SPRi biosensor for miRNA detection. With the functional nucleic acid-based amplification strategy by employing SDA, and AuNP enhancement sandwich assemblies, as low as 45.45 pM target miRNA can be detected. The established miRNA

assay exhibits excellent specificity and reproducibility. This novel SPRi biosensor offers a highly effective platform for miRNA analysis and clinical diagnostics as an alternative way compared to these existing conventional methods. It may be further extended to detect and quantify a wider range of DNA and RNA analytes.

Acknowledgements This work was funded by the National Natural Science Foundation of China (NSFC, No. 21205098).

Compliance with ethical standards The authors declare that all procedures performed in studies involving human participants were in accordance with the ethical standards of the institutional and/or national research committee and with the 1964 Helsinki declaration and its later amendments or comparable ethical standards. This article does not contain any studies with animals performed by any of the authors. Informed consent was obtained from all individual participants included in the study.

References

- Bartel DP (2004) MicroRNAs: genomics, biogenesis, mechanism, and function. *Cell* 116(2):281–297
- Liang Y, Ridzon D, Wong L, Chen C (2007) Characterization of microRNA expression profiles in normal human tissues. *BMC Genomics* 8(1):1
- Bartel DP (2009) MicroRNAs: target recognition and regulatory functions. *Cell* 136:215–233
- Forrest AR, Kanamori-Katayama M, Tomaru Y, Lassmann T, Ninomiya N, Takahashi Y, Hoona MJL, Kubosakia A, Kaihoa A, Suzukia M, Yasudaa J, Kawaia J, Hayashizakia Y, Humec DA, Suzukia H (2010) Induction of microRNAs, mir-155, mir-222, mir-424 and mir-503, promotes monocytic differentiation through combinatorial regulation. *Leukemia* 24(2):460–466
- Tili E, Michaille JJ, Croce CM (2013) MicroRNAs play a central role in molecular dysfunctions linking inflammation with cancer. *Immunol Rev* 253(1):167–184
- Jurkovicova D, Magyerkova M, Kulcsar L, Krivjanska M, Krivjansky V, Gibadulinova A, Oveckova I, Chovanec M (2014) miR-155 as a diagnostic and prognostic marker in hematological and solid malignancies. *Neoplasma* 61(3):241–251
- Várallyay É, Burgyán J, Havelda Z (2008) MicroRNA detection by northern blotting using locked nucleic acid probes. *Nat Protoc* 3(2):190–196
- Castoldi M, Schmidt S, Benes V, Hentze MW, Muckenthaler MU (2008) Michip: an array-based method for microRNA expression profiling using locked nucleic acid capture probes. *Nat Protoc* 3:321–329
- Chen CF, Ridzon DA, Broomer AJ, Zhou ZH, Lee DH, Nguyen JT, Barbisin M, Xu NL, Mahuvakar VR, Andersen MR, Lao KQ, Livak KJ, Guegler KJ (2005) Real-time quantification of microRNAs by stem-loop RT-PCR. *Nucleic Acids Res* 33:e179
- Kroh EM, Parkin RK, Mitchell PS, Tewari M (2010) Analysis of circulating microRNA biomarkers in plasma and serum using quantitative reverse transcription-PCR (qRT-PCR). *Methods* 50:298–301
- Bartosik M, Hrstka R, Palecek E, Vojtesek B (2014) Magnetic bead-based hybridization assay for electrochemical detection of microRNA. *Anal Chim Acta* 813:35–40

12. Cissell KA, Rahimi Y, Shrestha S, Hunt EA, Deo SK (2008) Bioluminescence-based detection of microRNA, miR21 in breast cancer cells. *Anal Chem* 80:2319–2325
13. Cheng Y, Lei JP, Chen YL, Ju HX (2014) Highly selective detection of microRNA based on distance-dependent electrochemiluminescence resonance energy transfer between CdTe nanocrystals and Au nanoclusters. *Biosens Bioelectron* 51:431–436
14. Bi S, Cui YY, Li L (2013) Dumbbell probe-mediated cascade isothermal amplification: a novel strategy for label-free detection of microRNAs and its application to real sample assay. *Anal Chim Acta* 760:69–74
15. Ye LP, Hu J, Liang L, Zhang CY (2014) Surface-enhanced Raman spectroscopy for simultaneous sensitive detection of multiple microRNAs in lung cancer cells. *Chem Commun* 50:11883–11886
16. Homola J (2008) Surface plasmon resonance sensors for detection of chemical and biological species. *Chem Rev* 108:462–493
17. Šípová H, Homola J (2013) Surface plasmon resonance sensing of nucleic acids: a review. *Anal Chim Acta* 773:9–23
18. Rich RL, Myszka DG (2000) Advances in surface plasmon resonance biosensor analysis. *Curr Opin Biotechnol* 11:54–61
19. Lausted C, Hu Z, Hood L, Campbell CT (2009) SPRi for high throughput, label-free interaction analysis. *Comb Chem High Throughput Screen* 12(8):741–751
20. Campbell CT, Kim G (2007) SPR microscopy and its applications to high-throughput analyses of biomolecular binding events and their kinetics. *Biomaterials* 28(15):2380–2392
21. Wu J, Huang Y, Bian X, Li D, Cheng Q, Ding S (2016) Biosensing of BCR/ABL fusion gene using an intensity-interrogation surface plasmon resonance imaging system. *Opt Commun* 377:24–32
22. Ding X, Yan Y, Li S, Zhang Y, Cheng W, Cheng Q, Ding S (2015) Surface plasmon resonance biosensor for highly sensitive detection of microRNA based on DNA super-sandwich assemblies and streptavidin signal amplification. *Anal Chim Acta* 874:59–65
23. He P, Qiao W, Liu L, Zhang S (2014) A highly sensitive surface plasmon resonance sensor for the detection of DNA and cancer cells by a target-triggered multiple signal amplification strategy. *Chem Commun* 50(73):10718–10721
24. Shi C, Liu Q, Ma C, Zhong W (2013) Exponential strand-displacement amplification for detection of microRNAs. *Anal Chem* 86(1):336–339
25. Ren R, Leng C, Zhang S (2010) Detection of DNA and indirect detection of tumor cells based on circular strand-replacement DNA polymerization on electrode. *Chem Comm* 46(31):5758–5760
26. Yu TX, Cheng W, Li Q, Luo CH, Yan L, Zhang DC, Yin YB, Ding SJ, Ju HX (2012) Electrochemical immunosensor for competitive detection of neuron specific enolase using functional carbon nanotubes and gold nanoprobe. *Talanta* 93:433–438
27. Mirkin CA, Letsinger RL, Mucic RC, Storhoff JJ (1996) A DNA-based method for rationally assembling nanoparticles into macroscopic materials. *Nature* 382:607–609.32
28. Jain PK, Lee KS, El-Sayed IH, El-Sayed MA (2006) Calculated absorption and scattering properties of gold nanoparticles of different size, shape, and composition: applications in biological imaging and biomedicine. *J Phys Chem B* 110(14):7238
29. Ditlbacher H, Krenn JR, Felidj N, Lamprecht B, Schider G, Salemo M, Leitner A, Aussenegg FR (2002) Fluorescence imaging of surface plasmon fields. *Appl Phys Lett* 80:404
30. Ghosh SK, Pal T (2007) Interparticle coupling effect on the surface plasmon resonance of gold nanoparticles: from theory to applications. *Chem Soc Rev* 107(11):4797–4862
31. Zhang D, Yan Y, Cheng W, Zhang W, Li Y, Ju H, Ding S (2013) Streptavidin-enhanced surface plasmon resonance biosensor for highly sensitive and specific detection of microRNA. *Microchim Acta* 180(5–6):397–403
32. Liu T, Chen X, Hong CY, Xu XP, Yang HH (2014) Label-free and ultrasensitive electrochemiluminescence detection of microRNA based on long-range self-assembled DNA nanostructures. *Microchim Acta* 181(7–8):731–736
33. Liu L, Jiang S, Wang L, Zhang Z, Xie G (2015) Direct detection of microRNA-126 at a femtomolar level using a glassy carbon electrode modified with chitosan, graphene sheets, and a poly(amidoamine) dendrimer composite with gold and silver nanoclusters. *Microchim Acta* 182(1–2):77–84
34. Wang M, Shen B, Yuan R, Cheng W, Xu H, Ding S (2015) An electrochemical biosensor for highly sensitive determination of microRNA based on enzymatic and molecular beacon mediated strand displacement amplification. *J Electroanal Chem* 756:147–152
35. Wang M, Yang Z, Guo Y, Wang X, Yin H, Ai S (2015) Visible-light induced photoelectrochemical biosensor for the detection of microRNA based on Bi₂S₃ nanorods and streptavidin on an ITO electrode. *Microchim Acta* 182(1–2):241–248